SANDIA REPORT

SAND2005-70362488
Unlimited Release
Printed July 2005

Active Mixing in Microchannels using Surface Acoustic Wave Streaming on Lithium Niobate

Darren W. Branch, Grant D. Meyer, Christopher J. Bourdon and Harold G. Craighead

Prepared by
Sandia National Laboratories
Albuquerque, New Mexico 87185 and Livermore, California 94550

Sandia is a multiprogram laboratory operated by Sandia Corporation,
a Lockheed Martin Company, for the United States Department of Energy's
National Nuclear Security Administration under Contract DE-AC04-94AL85000.

Issued by Sandia National Laboratories, operated for the United States Department of Energy by Sandia Corporation.

Available to DOE and DOE contractors from
U.S. Department of Energy
Office of Scientific and Technical Information
P.O. Box 62
Oak Ridge, TN 37831

Telephone: (865)576-8401
Facsimile: (865)576-5728
E-Mail: reports@adonis.osti.gov
Online ordering: http://www.osti.gov/bridge

Available to the public from
U.S. Department of Commerce
National Technical Information Service
5285 Port Royal Rd
Springfield, VA 22161

Telephone: (800)553-6847
Facsimile: (703)605-6900
E-Mail: orders@ntis.fedworld.gov
Online order: http://www.ntis.gov/help/ordermethods.asp?loc=7-4-0#online

SAND2005-70367036J
Unlimited Release
Printed July 2005

Active Mixing in Microchannels using Surface Acoustic Wave Streaming on Lithium Niobate

Darren W. Branch
Microsensor Science and Technology Department
Sandia National Laboratories
PO Box 5800
Albuquerque, NM 87185-1425

Christopher J. Bourdon
Thermal, Fluid, and Aero Experimental Sciences

Grant D. Meyer and Harold G. Craighead
Cornell University
School of Applied Physics
212 Clark Hall
Ithaca, NY 14853-3501

ABSTRACT

We present an active method for mixing fluid streams in microchannels at low Reynolds number with no dead volume. To overcome diffusion limited mixing in microchannels, surface acoustic wave streaming offers an extremely effective approach to rapidly homogenize fluids. This is a pivotal improvement over mixers based on complex 3D microchannels which have significant dead volume resulting in trapping or loss of sample. Our micromixer is integrable and highly adaptable for use within existing microfluidic devices. Surface acoustic wave devices fabricated on 128° YX $LiNbO_3$ permitted rapid mixing of flow streams as evidenced by fluorescence microscopy. Longitudinal waves created at the solid-liquid interface were capable of inducing strong nonlinear gradients within the bulk fluid. In the highly laminar regime (Re = 2), devices achieved over 93% mixing efficacy in less than a second. Micro-particle imaging velicometry was used to determine the mixing behavior in the microchannels and indicated that the liquid velocity can be controlled by varying the input power. Fluid velocities in excess of 3 $cm \cdot s^{-1}$ were measured in the main excitation region at low power levels (2.8mW). We believe that this technology will be pivotal in the development and advancement of microfluidic devices and applications.

CONTENTS

I. Introduction 5
II. Design and Fabrication 7
III. Experimental Setup and Procedure 10
IV. Results 14
V. Discussion 18
VI. Conclusion 20
References 21
Distribution List 25

I. INTRODUCTION

A major challenge in microfluidic systems is to overcome diffusion-limited processes within microchannels both in flow and static conditions. Microfluidic systems are now in widespread use for a host of applications including biochemical analysis [1], drug screening [2], biosensors [3], chemical reactions [4], cell sorting [5], sequencing of nucleic acids [6], and transport of small volumes of materials [7, 8]. At reasonable pressures flow is laminar and characterized by low Reynolds number. Mixing improves the dispersion control along the direction of Poiseuille flow. Moreover, the mixing time in solutions containing macromolecules, and other larger particles (e.g. superparamagnetic beads or latex particles) increases from seconds to hours in comparison to proteins. Consequently, high throughput systems and sensors that demand analysis in seconds to minutes require convective transport.

Several strategies exist to overcome diffusion limited mixing in microfluidic systems. One such strategy is to simply reduce the channel dimensions to a few micrometers, allowing molecular diffusion to mix the fluid streams in a few seconds. In fact, very rapid mixing times (<100μs) have been achieved using nozzles of a few micrometers [9], however large pressure drops and potential channel clogging prohibit use in many applications. In most cases, reducing the scale alone is not an option due to decreased fluid volume throughput and fouling issues. Integrating this approach is not typically an option in current microfluidic systems and hence other mixing strategies must be implemented.

Mixing strategies fall into two categories: passive and active. The general approach in both cases has been to increase the flux of the material between adjacent flow streams by decreasing the length and increasing the contact area over which diffusion occurs. Passive mixing relies on forcing liquids through fixed geometries to increase the interfacial area between the fluids by folding and stretching the fluid. Multiple stage laminations and flow splitting have been used to increase dramatically the interfacial area [10, 11]. Recently, chaotic advection has been used to achieve seemingly random and chaotic particle trajectories within fluid channels. Such passive mixers employ complicated three-dimensional serpentine twisted channels [12-14], however to date each lacks efficiency at low Reynolds number ($Re < 1$). More recently, a passive mixer using bas-relief features has been demonstrated [15] providing efficacious mixing even at low Reynolds number. The bas-relief structure was used to generate transverse flows in the microchannel such that liquid

streams twisted over one another. One disadvantage is that in order to generate the chaotic-advection required for mixing, complex three-dimensional microstructures often must be fabricated. These structures contain dead volume and may easily foul when using complex solutions.

In contrast, active mixing is achieved through periodic perturbation or chaotic-advection of the flow fields. Unlike passive devices, active mixers require external power sources and hence slightly more complex packaging methods. As a tradeoff for system complexity, active mixers typically outperform their passive counterparts especially under highly laminar conditions (Re << 1). Several fluid actuation methods have been demonstrated, including heat convection [16], differential pressure [17-19], vapor pneumatic power [20], magnetic actuation [21], electrowetting [22], electrokinetic pressure [23, 24], and ultrasonic actuation [25-28]. A distinct advantage of active mixers is the ability to mix in the absence of flow, which assures that chemical reaction times are faster than residence times in the microchannels.

It is well known that ultrasonic actuation can significantly influence the pressure variation within fluids. Acoustic pressure variation can be large enough to cause cavitation, where the pressure forces exceed the intermolecular cohesion forces. Though bubble formation and collapse can induce mixing, a secondary mechanism exists where the acoustic energy is dissipated by viscous stress. This phenomenon is called *acoustic streaming*. It has been shown that a*coustic streaming* can generate large nonlinear gradients within fluids [29, 30]. Acoustic micromixers have produced liquid oscillations using thickness-mode resonances in zinc oxide (ZnO) [31], induced ultrasonic vibration of thin silicon membranes to actively mix fluids using lead-zirconate-titanate (PZT) [27, 32], and moved liquid droplets using 128° YX $LiNbO_3$. In contrast to the micro-machined silicon openings of Zhu *et al.*, Yang *et al.* devised a closed chamber for mixing, permitting the device to be used as an active micromixer [27, 31]. Early studies that used 128° YX $LiNbO_3$ only considered SAW streaming in open systems [33, 34]. Though these studies clearly demonstrate acoustic streaming, these devices must be integrated in closed chambers to prevent evaporation and for device portability.

In this study, we investigate an active micromixer based on the surface acoustic wave streaming (SAWS) phenomenon on 128° YX $LiNbO_3$. This device differs from previous

streaming devices, in that we have integrated microchannels onto the device to confine the liquid flow and prevent sample evaporation. When a SAW from 128° YX $LiNbO_3$ reaches a solid/liquid boundary, the Rayleigh wave becomes leaky, exciting longitudinal waves into the liquid at an angle of ca. 23° to the surface normal [35]. This phenomenon can be used to produce very efficient acoustic streaming [30]. Of significance is that the electromechanical coupling constant for 128° YX $LiNbO_3$ (K^2 = 5.5%) is much higher than quartz, ZnO, or aluminum nitride (AlN) (0.16, 1.1, [35] and 0.4% [36], respectively), which also generate Rayleigh waves. Assessment of micromixer performance was performed using micro-particle velicometry (μPIV), which has been proven to be powerful in the determination of fluid velocity mapping within channels. Fluid velocity was measured as a function of the power delivered to the mixer to determine optimal operating conditions. To assess mixing efficacy, fluorescence microscopy was used to actively monitor two separate flow streams as each passed through the acoustic mixing region. Microchannels were fabricated with dimensions required to produce Reynolds numbers on the order of one for highly laminar flow conditions. Device optimization and integration approaches for microfluidic systems were also explored.

II. DESIGN AND FABRICATION

To provide a platform to study surface acoustic wave mixing in microchannels, we evaluated two SAWS device designs for integration with microfluidic channels. First, the fabrication of the SAWS devices will be described, followed by a description of the microfluidic channels, and finally a description of the integrated device for fluorescence microscopy and particle imaging velicometry.

The SAWS devices were fabricated using single-side polished 128° YX $LiNbO_3$ (Crystal Technology, Inc., Palo Alto, CA) wafers that were pre-cleaned by rinsing with acetone, methanol, isopropanol, and 18 MΩ·cm water, respectively then dried with N_2. A lift-off procedure was used to define the IDTs. To promote adhesion, a 100 Å chromium (Cr) binding layer was evaporated on the $LiNbO_3$ wafers using an e-beam evaporator (CVC Products, Inc.). A 900 Å gold layer was then deposited on the Cr film by resistive evaporation. To protect the IDT patterns during dicing, AZ4110 photoresist was applied to wafers and then baked at 90 ºC for 90 sec. Prior to dicing, the fine-ground side of the wafer

was mounted on blue medium tack (Semiconductor Equipment Corp., Mesa, AZ). The wafers were then diced with a 1.8 mm width wheel, using a feed rate of 0.2 $mm \cdot s^{-1}$, and a spindle speed of 12,000 rpm. Two IDT layouts were fabricated to evaluate the efficiency of the SAWS devices: 1) a *bidirectional double split finger* IDT (Fig. 1a) and 2) a bidirectional double split finger IDT with an *acoustic horn* to compress the Rayleigh (Fig. 1b) waves. The active mixing region was defined between IDTs patterned on the $LiNbO_3$ wafers, creating region permissible for microfluidic flow using a wide range of channel dimensions. The bidirectional IDTs consisted of 56 finger pairs with an aperture of 38λ and a metallization ratio of $\eta = 0.5$. The IDT center-to-center separation was 120λ. The acoustic horn compressed the Rayleigh beam (aperture 12λ) by a factor of four to facilitate localized mixing within the microfluidic channels. Both IDT layouts supported Rayleigh waves with a center frequency of 90 MHz, having an insertion loss ranging from -7 to -10 dB.

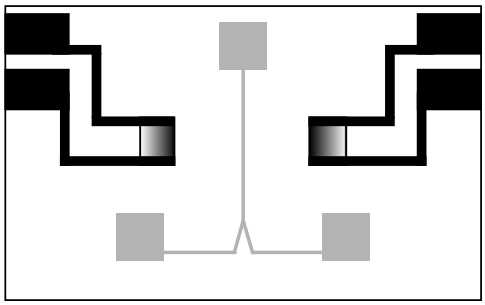

Fig. 1a. Bidirectional double split finger IDT design. The electrical ports are shown in black and the IDTs are shown as black-white gradients. The gray region shows the position of the Y-junction, creating the fluidic interface.

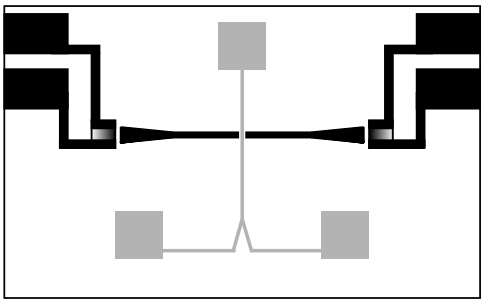

Fig. 1b. Bidirectional double split finger IDT with an *acoustic horn.* The acoustic horn was used to compress the Rayleigh waves to increase the power density by a factor of four.

To evaluate the performance of the SAW micromixer, we fabricated two microfluidic channels. Both channels were designed to achieve low Reynolds numbers ($Re < 2$). The slightly larger microchannel facilitated the μPIV analysis. We used Y-junction layout to create a fluidic interface in the acoustic excitation region (Fig. 1a and 1b). In order to fabricate the microfluidic channels, silicon molds were selectively etched with a Unaxis SLR 770 ICP deep reactive ion etcher (DRIE). The silicon molds were etched with a width, height, and length of 50 μm, 110 μm, and 4 mm, respectively.

For rapid prototyping, polydimethylsiloxane (PDMS) was poured into the silicon molds to create the Y-junction microchannels. The PDMS microchannels were cast using a 1:10 (wt/wt) mixture of Sylgard silicone and silicone elastomer 184 (Dow Corning Corporation). Fluidic connections were cast directly into the PDMS using silicone rubber (VWR Inter., West Chester, PA) tubing and a Delrin® fixture to hold the tubing in place (Fig. 2a). For the integrated device, the PDMS microfluidic channels were attached to $LiNbO_3$ substrates by heating the substrate to 90°C, followed by immediate contact. The microchannel was aligned to mate with the center of the acoustic excitation region. However, the expected acoustic loss from using microchannels fabricated entirely from PDMS can result in significant attenuation. This issue was addressed by fabricating microfluidic channels from polycarbonate and through minimizing the contact area of the PDMS seal with the $LiNbO_3$ substrate (Fig. 2b). The polycarbonate viewing region was polished using dichloromethane vapor for optical interrogation of the fluid flow. The polycarbonate microchannels had a width, height, and length of 750 μm, 510 μm, and 7.6 mm, respectively. At these dimensions, a Reynolds number of less than one was attainable. The polycarbonate microchannels were used to asses the mixing efficacy of fluids during the μPIV analysis.

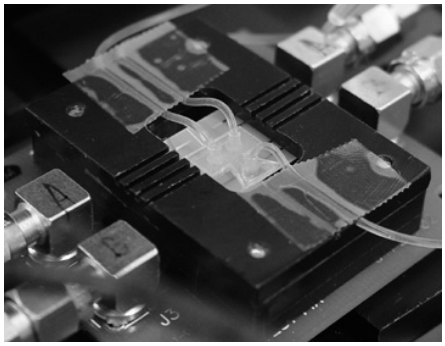

Fig. 2a. PDMS microfluidic channels were bonded to the $LiNbO_3$. Microchannels cast using PDMS had a 50 μm width, 110 μm height, and a 4mm length. The fluidic connections were attached to grooves in a Delrin® lid.

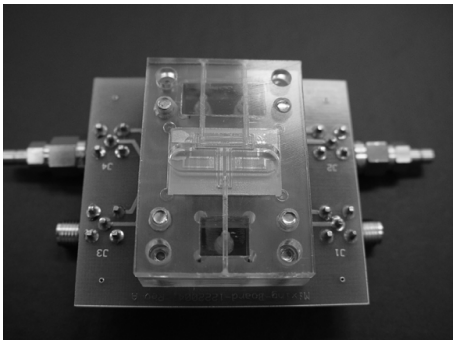

Fig. 2b. Polycarbonate microfluidic channel were attached to $LiNbO_3$ using PDMS seals. The polycarbonate flow channels had a width, height, and length of 750 μm, 510 μm, and 7.6 mm, respectively.

Surface acoustic wave streaming produces strong radiation forces acting on fluids and particles suspended in the fluids. To estimate the force acting on particles in solution we begin by solving the equation of motion for a solution of microspheres in an ultrasonic field.

The solution of the velocity field can be written as

$$v(t) = \frac{F_{ac}}{6\pi\eta r}\left(1 - e^{\frac{-6\pi\eta r}{m}t}\right) \quad (1)$$

where F_{ac} is the net acoustic radiation force due on the microsphere, η is the fluid viscosity, and m is the particle mass. In general, F_{ac} describes the net force on the microspheres due to acoustic wave streaming and hence fluid motion. We used Stokes drag relationship to derive (1), which is a reasonable assumption when Re < 0.5. For the case when equilibrium is reached $t \to \infty$, (1) becomes

$$v(t) = \frac{F_{ac}}{6\pi\eta r} \quad (2)$$

Equation (2) permits estimation of the net acoustic radiation pressure acting on the microspheres in the fluid.

III. Experimental Setup and Procedure

In previous studies, mixing efficacy has been evaluated using fluorescent dyes [11, 13, 15, 16, 18, 37], pH indicators [12, 31], and color dyes [21, 27]. We have chosen to use the fluorescent dye Alexa-488, which is insensitive to pH between pH 4 and 10 and has superior quantum yield to fluorescein dyes. Since inks and dyes do not show any chemical reaction when mixed, proportional mixing can be observed within the microchannels.

We evaluated the ability of the SAWS device to mix two fluidic streams by employing a Y-junction microchannel fabricated in PDMS. After fabrication, the SAWS devices were mounted in a Delrin® fixture containing AlphaTest *μHELIX*® test probes (AlphaTest Corporation, Mesa, AZ). The top surface of this fixture was fabricated with grooves as means of strain relief for the silicon rubber tubing connections (Fig. 2a). This assembly was positioned on the stage of an Olympus IX-70 microscope (Olympus America, Melville, NY). The emission (535 nm) was selected using an Alexa-488 filter (Chroma Scientific, Rockingham, VT). One stream contained a 100 mM PBS buffer pH 7.4 and the second contained 250 μg ml^{-1} protein-A (Sigma, St. Louis, MO) conjugated with Alexa-488 dye (Molecular Probes Inc., Eugene, OR) dissolved in 100 mM PBS buffer pH 7.4. The two

streams were introduced from syringes connected by PMMA tubing (Upchurch Scientific, Oak Harbor, WA) attached to the silicone rubber tubing connectors on the PDMS microchannels. A PHD 2000 Harvard Apparatus syringe pump (Harvard Apparatus Inc., Holliston, MA) was used to control the volumetric flow rate.

The SAWS devices were driven using an HP 8656 RF signal generator (Agilent Technologies, Palo Alto, CA). The signal was then amplified with an ENI 420LA 20W RF power amplifier (Bell Electronics, Kent WA) and split using a 50Ω power divider. The amplified signal provided power to both IDTs simultaneously during the mixing experiments. Output power was controlled by varying the input signal level of the HP 8656 RF signal generator through software control. To account for transmission losses in the setup, we measured the overall system gain using an HP 8508 vector voltmeter (Agilent Technologies, Palo Alto, CA). The actual power delivered to the SAWS devices were determined by measuring the return loss of each transducer. This permitted evaluation of the true power delivered to each of the micromixer devices. The complete setup used to perform the mixing experiments is schematically represented in Fig. 3.

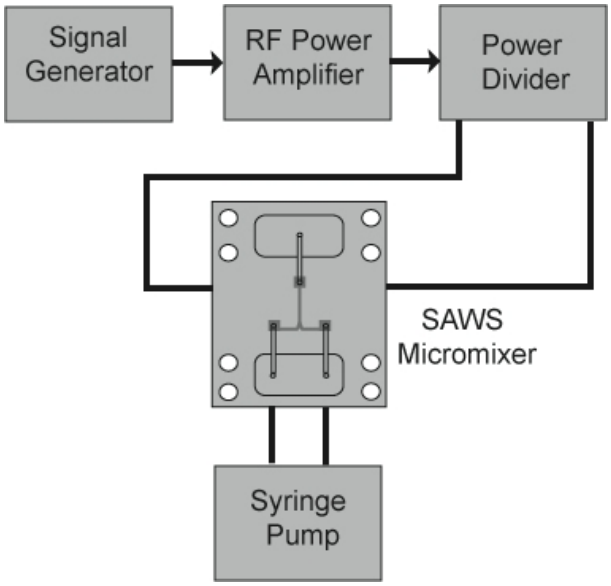

Fig. 3. Schematic shows the electrical and fluidic connections to the SAWS micromixers. The SAWS micromixer fixture was fabricated from polycarbonate and polished for optical interrogation of the fluidic microchannel.

The mixing efficacy was quantified by measuring the fluorescence intensity across the area of the microchannel. Video images captured with a Retiga 1300 12-bit CCD camera (QImaging, Burnaby, B.C. Canada) were converted into sequential 640 x 480 TIFF-formatted images using Qcapture Pro Software (QImaging, Burnaby, B.C. Canada). The fluorescent images were converted into a three-slice RGB stack, using the green slice to build a monotone spectrum. Color index ranged from 255 for black to 0 for green. The spatial-temporal variation of color in the microchannel was analyzed using the image-processing toolbox from Matlab®. The 12-bit

images were processed by determining the color index for sets of pixels in the captured images. For the mixing analysis, we used the standard deviation of color index to determine the mixing index (α) as

$$\alpha = \sqrt{\frac{1}{N}\sum_{i=1}^{N}\left[\frac{C_i - \bar{C}}{\bar{C}}\right]^2} \tag{3}$$

The color index is specified by C_i at pixel i and $\bar{C}$ is the average over N pixels in the sampling region. For a homogeneous mixture within the microchannel, the value of α approaches zero. We used this measure to determine the mixing index in the microchannel at sampled regions downstream from the acoustic excitation region. Intensity variation in the images due to the CCD and lighting was corrected by normalizing the raw images before computing the mixing index (i.e. $\|C_i\| = 1$). Though homogeneous mixtures would ideally have $\alpha \rightarrow 0$, the fluorescence variation of a uniform region often produces a noise floor above 0. We estimated this noise floor (α_n) by measuring the background fluorescence variation of a uniform section of the fluorescence in the flow region. Based on this analysis, a well-mixed solution would approach α_n across the length of the microchannel. All microchannels were imaged at the midpoint (h/2 = 55 μm) depth of field.

To map the fluid flow and velocities within the microchannels during surface acoustic wave streaming, we used μPIV to characterize flow in the microchannels. μPIV is a velocity measurement technique that extracts instantaneous two-dimensional fluid velocity information from within micro-devices by tracking the motion of small, fluorescent tracer particles. This technique is capable of micron-resolution in-plane and 2-3 micron resolution out-of-plane. To couple the μPIV with our microchannel, we used the polycarbonate flow cell in Fig. 4 to permit optical interrogation of the microchannels. The SAWS devices were placed above the objective of an epi-fluorescent microscope. Light from a Nd:YAG laser (532 nm) enters the microscope through an aperture on the back of the microscope and is focused onto a small region of the microfluidic device by the imaging objective, illuminating the entire depth of the fluid. This illumination technique only requires one side of the microfluidic device to be optically accessible. Fluorescent microspheres (d_p = 1 μm, Duke

Scientific, Palo Alto, CA) displaying an excitation at peak at 532 nm and an emission at peak from 550-570 nm were used as tracers in all the μPIV experiments. Beads on the micrometer scale were used to reduce aberration and permit rapid assessment of particle trajectory. The emitted light from the particles as well as scattered and reflected laser light was filtered and captured using a Micro-Max 12-bit 1300 x 1300 CCD camera (Roper Scientific, Tucson, AZ) capable of capturing two frames within 200ns. Images were processed using a single-pass cross-correlation technique having non-overlapping 32x32 pixel windows to obtain the velocity field and acoustic streaming force data.

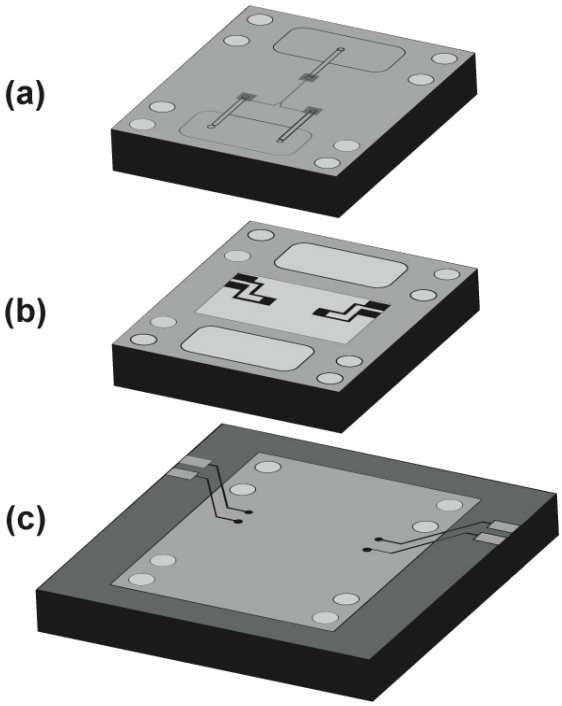

Fig. 4. Exploded view of the acoustic mixing fixture for μPIV analysis. The components were fabricated from polycarbonate. (a) Fluidic cap (b) Recessed polycarbonate insert supported the SAWS devices for simultaneous connection to the fluidic cap and AlphaTest *μHELIX*® test probes. (c) The PC Board connected the test probes to the SAWS devices in (b).

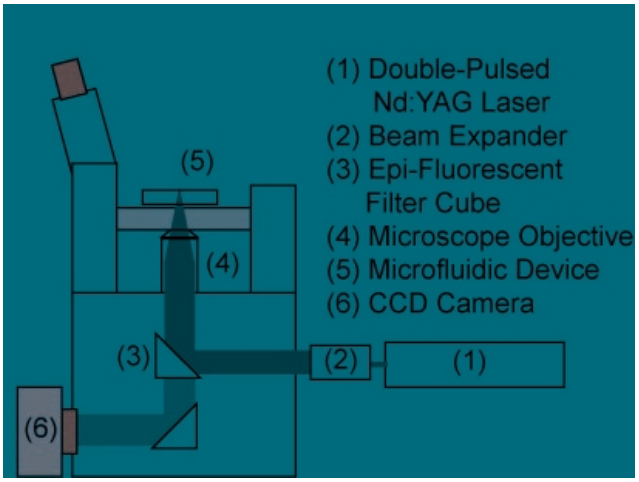

Fig. 5. Primary components of the μPIV system. The respective positions of the tracer particles were used to compute the associated fluid velocity and acoustic streaming forces.

IV. RESULTS

The efficacy of the surface acoustic wave streaming device to rapidly homogenize two fluids streams was assessed by quantifying the fluorescence intensity of protein-A labeled with Alexa-488 in the PDMS microchannels. We first evaluated the mixing efficacy for the bidirectional double split finger IDT shown in Fig. 1a. This SAWS micromixer had a beam width of 1.7 mm. The flow rate was set for 10 μl·min-1 giving a Reynolds number of 2.0 in the microchannel. In Fig. 6a the flow was observed to be highly laminar throughout the microchannel. By applying 100 mW to the micromixer at 90 MHz, we observed immediate and rapid mixing of the two flow streams (Fig. 6b). Mixing by diffusion was measured to take approximately 26 s, however at a flow rate of 3.1 cm·s-1, the contact time was ca. 0.13 s. This indicates that diffusion based mixing would require about 80 cm of flow to homogenize the two flow streams. With acoustic excitation, the interface between the two streams was rapidly homogenized (Fig 6b), resulting in continuous mixing of the two-laminar flow streams. Upon removal of acoustic excitation (Fig 6c), laminar flow was restored in ca. 0.13 s, which was approximately the residence time (channel length/average flow velocity) for fluid in the microchannel.

(a)

(b)

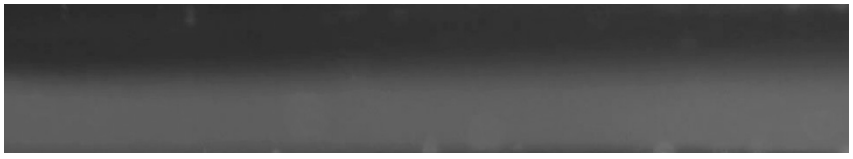

(c)

Fig. 6. Captured video frames showing acoustic mixing in the microchannel. The captured segment was 1 mm downstream from the acoustic excitation region, with the acoustic excitation 1mm downstream from the Y-junction. Fluid flow was from left to right at a rate of 10 μl·min^{-1}. The length of each segment was 350 μm.

The mixing index (α) determined by (3) was computed 1 mm downstream from the excitation region in the microchannel to determine the mixing efficacy. To estimate the noise floor (α_n) we measured the fluorescence variation in a region of uniform fluid flow (Fig. 6a). By computing α along the length of the microchannel, we determined the normalized fluorescent background variation to be ca. 0.10. This indicates that complete mixing would occur when $\alpha \leq 0.10$. Fig. 7 shows the mixing index sampled along the length of the microchannel in the presence and absence of acoustic excitation for laminar flow conditions. In the absence of mixing, the index was well above 0.50 throughout the entire microchannel. With acoustic excitation, the mixing index decreased to ca. 0.05 and was indistinguishable from noise floor throughout the entire microchannel (Fig. 7), corresponding to a mixing efficiency of 93%.

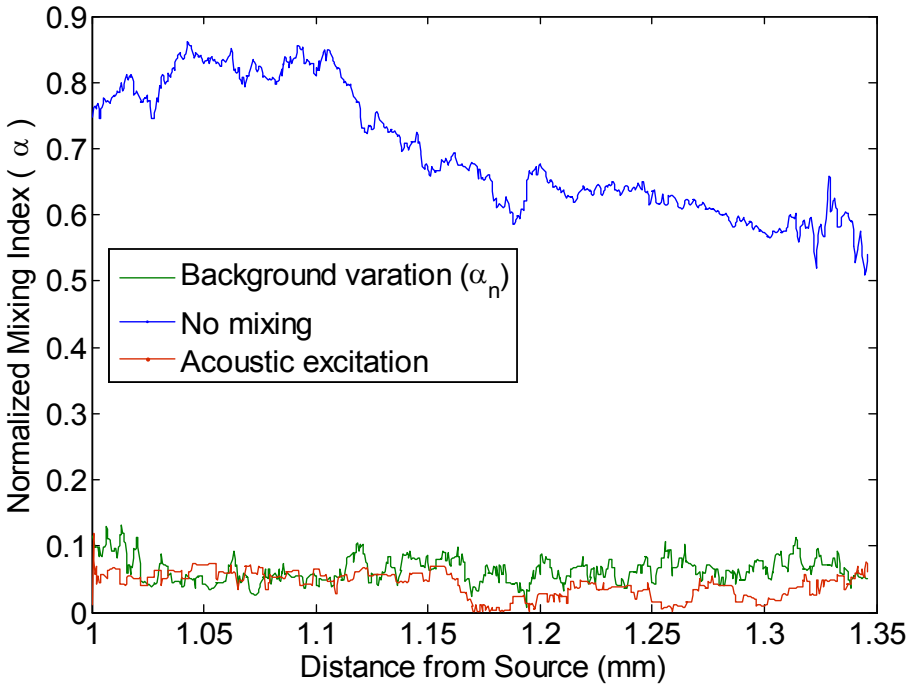

Fig. 7. Normalized mixing index (α) sampled along the length of the microchannel.

The acoustic horn (Fig. 1b) compressed a 500 μm beam width to 125 μm, giving a four-fold increase in power density. When using the acoustic horn layout, we determined

that only 20mW of power was required to achieve similar mixing results (Fig. 7). This result agrees reasonably well with fact that the power density is about four times greater in the acoustic horn excitation region (125 μm). Though the mixing region was only 125 μm in width, homogeneous mixing (α < 0.1) was observed throughout the microchannel, and required significantly less input power. The reduction of beam width had no appreciable effect on the overall homogeneity of mixing along the length of the microchannel.

To evaluate the fluid velocities due to surface acoustic wave streaming within the microchannels, we measured the velocity throughout the microchannel by acquiring slices in the z-plane. This was performed in the absence of external fluid flow to determine the fluid velocity attributed to SAWS. Fig. 8a-f shows velocity slices for three different power levels in the microchannels. Our results demonstrate fluid velocities in excess of 3 cm·s^{-1} near the excitation region for 4.5 dBm (3.2 mW) of input power for the *bidirectional* IDT. By using (2), we calculated an acoustic radiation pressure of 45 pN·m^{-2} when the flow velocity was 3 cm·s^{-1}. We observed highly non-uniform fluid velocities across the microchannels, as evidenced by the presence of fluidic sources and sinks. The fluid velocity tended to decrease further from the acoustic excitation region aside from recirculation effects. The lower slices (Fig. 8a,c,e) were captured 170 μm away from the $LiNbO_3$ substrate, with the upper slices (Fig. 8b,d,f) at 340 μm. Though the general dependence shows a strong velocity variation near the excitation regions, the fluid velocity was highly non-uniform in the sampled regions. By

(a) (b)

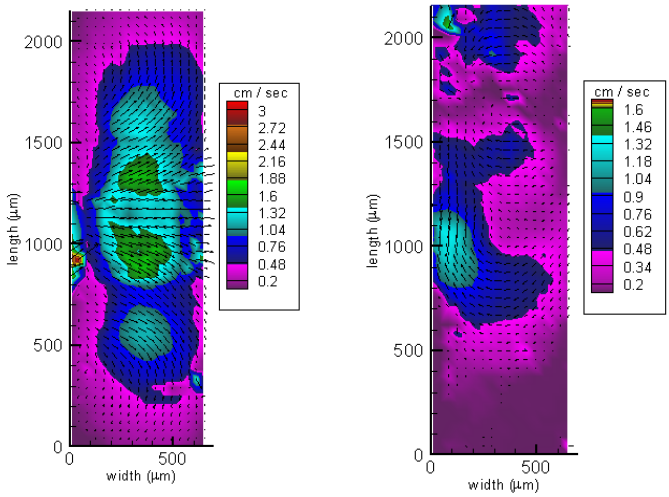

Fig. 8a-b. In the absence of external flow, μPIV data indicated rapid particle movement throughout the microchannel. The excitation region was 1.7 mm in length and centered at 1200 μm along the y-axis.

varying the total applied acoustic power, we determined the dependence of the fluid velocity on the input power accounting for return losses. Results in Fig. 9 indicated that 4.5 dBm (2.8 mW) produced fluid velocities in excess of 2 cm·s^{-1} with no observable acoustic cavitation. The mean fluid velocity was computed from μPIV data, which was sampled along the width of the *bidirectional* IDTs (38λ). For the acoustic horn (IDT aperture of 9.5λ), we observed that about a four-fold decrease in power to obtain fluid velocities shown in Fig. 9. This indicated that geometrical modifications can dramatically reduce power requirements, while maintaining mixing efficacy.

(c) (d) (e) (f)

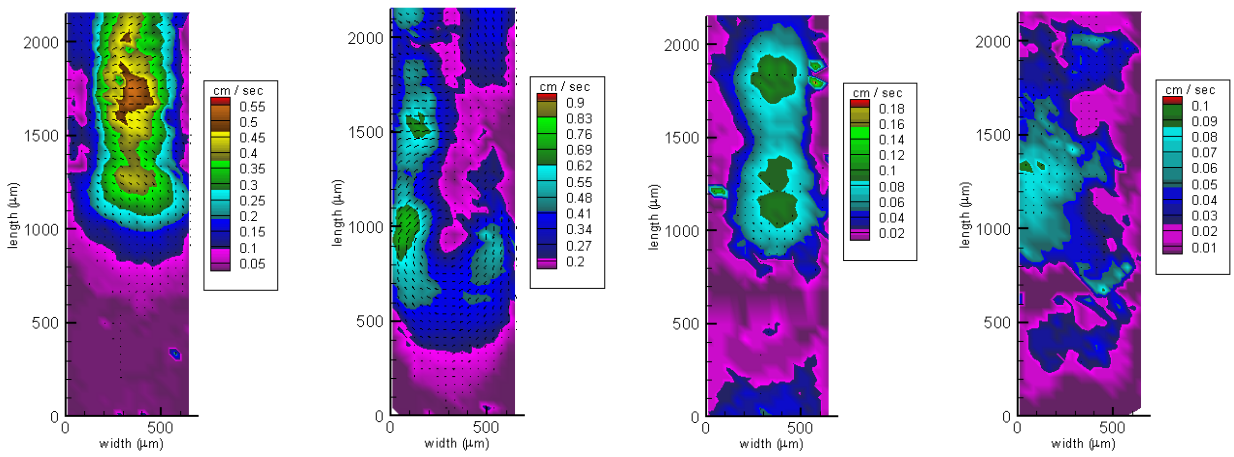

Fig. 8c-f. For (c) and (d) the total excitation power was -3.5 dBm (0.47 mW), where (e) and (f) were measured using an input power of -15.5 dBm (28 µW).

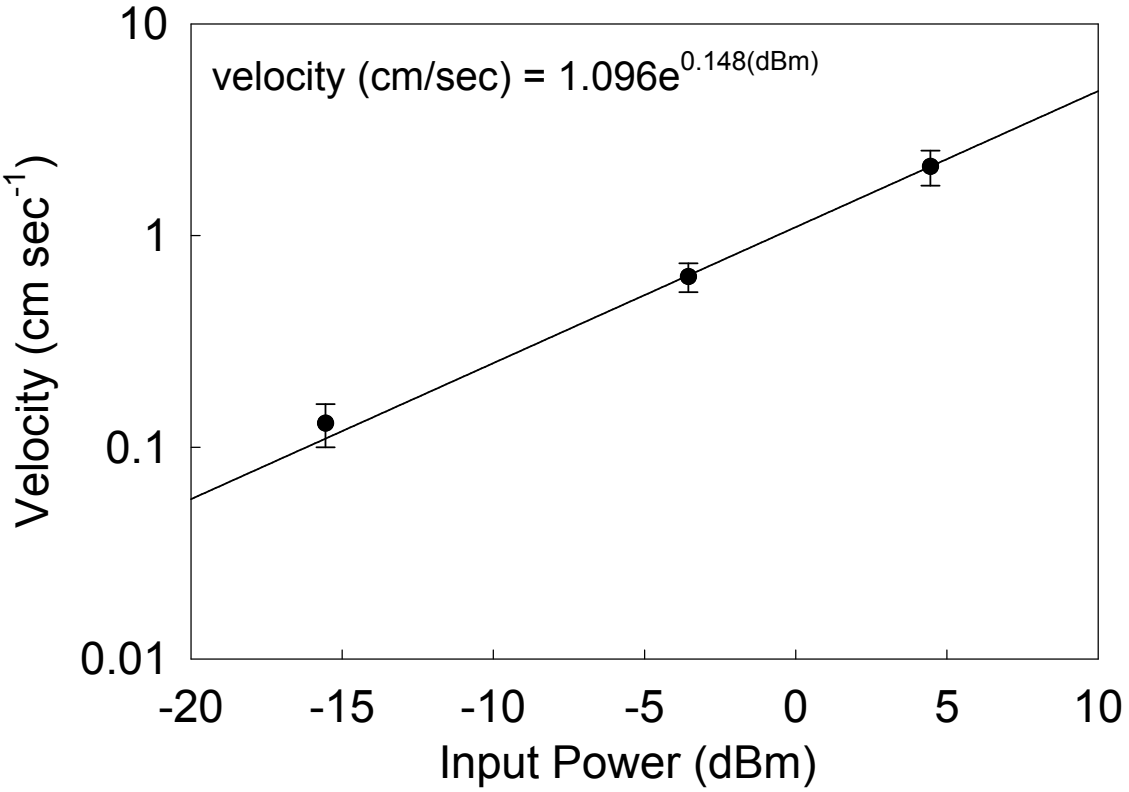

Fig. 9. Fluid velocity in the microchannels as a function of the total input power. The mean fluid velocity was determined from μPIV data by taking samples along the acoustic excitation source. The region was a line that covered the width of the IDT aperture inside the flow region and against the microchannel wall. We report the mean ± std. dev. (n=3) at each power level.

V. DISCUSSION

This study demonstrates the successful mixing of fluidic streams at low Reynolds numbers (Re ~ 2.0) by launching surface acoustic waves into microchannels. This method of excitation generates longitudinal waves in fluids, producing nonlinear fluid movement in the microchannels. During acoustic excitation the mixing was rapid and homogeneous throughout the microchannel. Principle to our method is the use of interdigital electrodes that launch Rayleigh waves into the microfluidic channels under a polycarbonate fluidic cap, permitting remote perturbation of the fluid. This approach is adaptable to a wide range of geometries, with integration into existing microfluidic devices. This is a crucial improvement over mixers based on complex 3D structures which suffer from dead volume, surface fouling, sample loss, and require pressure to drive fluidic flow.

Fluorescence analysis of microchannels containing protein-A labeled with Alexa-488 dye exhibited laminar behavior (Fig. 6a) as shown in the captured segment. The goal was to

establish laminar flow conditions representative of typical conditions encountered in microfluidic systems. We found that the mixing index (α) remained well above 50% throughout the length of the microchannel (Re = 2). Captured segments 1 mm downstream (Fig. 6) from the acoustic source remained strongly laminar. Laminar behavior was observed throughout the microchannel and it is useful to compute the mixing length given by, $Q \cdot \tau = 800\, mm$, where Q is the flow rate and τ is the measured diffusion time for the protein-A labeled Alexa-488 conjugate. This indicated that molecular diffusion for our flow conditions was insufficient to mix the streams over the region of our microchannels (length: 4mm). During acoustic excitation (Fig. 6), the fluid was rapidly homogenized, yielding a fluorescence response that was indistinguishable from the background fluorescence (Fig. 7) for a uniform segment of fluid flow. The homogenization was equivalent to the noise floor of the fluorescence background. This is conclusive evidence that a high degree of homogenization was achieved in the microchannels. Removal of excitation restored laminar flow in about 0.1 seconds, which was approximately the time required to replace the fluid volume.

The use of μPIV proved powerful in the determination of fluidic trajectories within the microchannels (Fig. 8). Our study required using larger microchannels (width: 750 μm, height: 510 μm, and length: 7.6mm) to facilitate the μPIV analysis. Microchannels fabricated from polycarbonate were polished to permit optical interrogation of the microchannels for acquisition of the flow field in real time. For the larger channels, the estimated time required for tracer particles to cross the width of the microchannel would be 710 μm / 4 cm·s^{-1} = 0.02 s Given the rapid frame capture time (200 ns) for the μPIV analysis, particle trajectories were sufficiently slower to permit two-dimensional interrogation. Difficulties were encountered for rapidly moving particle trajectories that were out of the focal plane, preventing capture of the coordinates.

Fluidic velocities decreased the further away from the excitation region (Fig. 8). Slices imaged at 170 μm from the source exhibited more uniform patterns in the fluid, whereas motion at 340 μm above the surface of the SAW was non-uniform. Even at very low power levels (28 μW), fluid velocities in excess of (0.1 cm·s^{-1}) were observed within the microchannels. Our analysis of fluid flow in the microchannels was restricted to two-

dimensional slices, given the large velocities we observed out of the focal plane. These results suggest that fluidic motion was highly complex, capable of folding and stretching laminar streams to produce excellent mixing. A possible improvement in our approach would be to capture the three-dimensional fluid flow during surface acoustic wave streaming. Further analysis would then permit computation of lyapunov exponents through time-averaged projection of particle motions. Our results showed that the fluid velocity near the acoustic excitation region can be specified by the input power. In Fig. 9, fluid velocities can be predicted based on the applied power input. This permits selection of appropriate power requirements to achieve the desired fluid velocities and mixing behavior.

VI. CONCLUSION

We investigated SAWS as a method to mix fluids within microchannels, where laminar flow is the dominant flow behavior. Our results show that SAWS devices can be applied to produce highly efficient mixing within microchannels. This approach has several key advantages over existing methods in that it permits remote actuation, has an on/off mixing capability, eliminates dead volume, and can be operated with low power.

The widespread use of microfluidic systems demands that mixing strategies are easily incorporated to overcome diffusion limited processes. This is crucial to improve kinetics for rapid biochemical analysis or when using fluids such as blood, where protein content fouls with other mixing devices. In these situations, mixing enhancement strategies are crucial to perturb the laminar flow to achieve folding of the fluid, allowing molecular diffusion to complete the process. We believe that surface acoustic wave streaming will be a powerful method to overcome diffusion limited processes, significantly improving existing microfluidic systems.

REFERENCES

[1] C. Bisson, J. Campbell, R. Cheadle, M. Chomiak, J. Lee, C. Miller, C. Milley, P. Pialis, S. Shaw, W. Weiss, and C. Widrig, "A microanalytical device for the assessment of coagulation parameters in whole blood," presented at Proc. Solid-State Sens. Actuator Workshop, Hilton Head, SC, 1998.

[2] N. Chiem, C. Colyer, and J. D. Harrison, "Microfluidic systems for clinical diagnosis," presented at Proc. Int. Solid-State Sens. Actuators Conf., Chicago, IL, 1997.

[3] E. Eteshola and D. Leckband, "Development and characterization of an ELISA assay in PDMS microfluidic channels," *Sensors and Actuators B*, vol. 72, pp. 129-133, 2001.

[4] M. W. Losey, M. A. Schmidt, and K. F. Jensen, "Microfabricated multiphase packed-bed reactors: Characterization of mass transfer and reactions," *Ind. Eng. Chem. Res.*, vol. 2001, pp. 2555-2562, 2001.

[5] H.-P. Chou, C. Spence, A. Scherer, and S. Quake, "A microfabricated device for sizing and sorting of DNA molecules," *Pro. Natl. Acad. Sci. U.S.A.*, vol. 96, pp. 11-13, 1999.

[6] M. A. Burns, B. N. Johnson, S. N. Brahmasandra, K. Handique, J. W. Webster, M. Krishnan, T. S. Sammarco, P. M. Man, D. Jones, D. Heldsinger, C. H. Mastrangelo, and D. T. Burke, "An integrated nanoliter DNA analysis device," *Science*, vol. 282, pp. 484-487, 1998.

[7] Y. Mizukami, D. Rajniak, A. Rajniak, and M. Nishimura, "A novel microchip for capillary electrophoresis with acrylic microchannel fabricated on photosensor array," *Sensors and Actuators B*, vol. 81, pp. 202-209, 2002.

[8] O. T. Guenat, D. Ghiglione, W. E. Morf, and N. F. d. Rooij, "Partial electroosmotic pumping in complex capillary systems Part 2: Fabrication and application of a micro

total analysis system (μTAS) suited for continous volumetric nanaotitrations," *Sensors and Actuators B*, vol. 72, pp. 273-282, 2001.

[9] J. B. Knight, A. Vishwanath, J. P. Brody, and R. H. Austin, "Hydrodynamic focusing on a silicon chip: Mixing nanoliters in microseconds," *Phys. Rev. Lett.*, vol. 80, pp. 3863-3866, 1998.

[10] J. Branebjerg, P. Gravesen, J. P. Krog, and C. R. Nielsen, "Fast mixing by lamination," presented at Proc. IEEE MEMs Workshop, San Diego, CA, 1996.

[11] N. Schwesinger, T. Frank, and H. Wurmus, "A modular microfluid system with an integrated micromixer," *J. Micromech. Microeng.*, vol. 6, pp. 99-102, 1996.

[12] R. H. Liu, M. A. Stremler, K. V. Sharp, M. G. olsen, J. G. Santiago, R. J. Adrian, H. Aref, and D. J. Beebe, "Passive mixing in a three-dimensional serpentine microchannel," *J. Microelectromechan. Sys.*, vol. 9, pp. 190-197, 2000.

[13] D. J. Beebe, R. J. Adrian, M. G. Olsen, M. A. Stremler, H. Aref, and B.-H. Jo, "Passive mixing in microchannels: Fabrication and flow experiments," *Mec. Ind.*, vol. 2, pp. 343-348, 2001.

[14] R. A. Vijayendran, K. M. Motesgood, D. J. Beebe, and D. E. Leckband, "Evaluation of a three-dimensional micromixer in a surface-based biosensor," *Langmuir*, vol. 19, pp. 1824-1828, 2003.

[15] A. D. Stroock, S. K. W. Dertinger, A. Ajdari, I. Mezic, H. A. Stone, and G. M. Whitesides, "Chaotic mixer for microchannels," *Science*, vol. 295, pp. 647-651., 2002.

[16] J. W. Choi and C. H. Ahn, "An active micro mixer using electrohydrodynamic (EHD) convection," presented at Proc. Solid-State Sens and Actuators Workshop, Hilton Head Island, SC, 2000.

[17] K. Hosokawa, T. Fujii, and I. Endo, "Droplet-based nano/picoliter mixer using hydrophobic microcapillary vent," presented at Proc. IEEE MEMs Workshop, Orlando, FL, 1999.

[18] J. Voldman, M. L. Gary, and M. a. Schimdt, "An integrated liquid mixer/valve," *J. Microelectromechan. Sys.*, vol. 9, pp. 295-302, 2000.

[19] J.-H. Tsai and L. Lin, "Active microfluidic mixer and gas bubble filter driven by thermal bubble micropump," *Sensors and Actuators A*, vol. 97-98, pp. 665-671, 2002.

[20] J. Evans, D. Liepmann, and A. P. Pisano, "Planar laminar mixer," presented at Proc. IEEE MEMS Workshop, Nagoya, Japan, 1997.

[21] L.-H. Lu, K. S. Ryu, and C. Liu, "A magnetic microstirrer and array for microfluidic mixing," *J. Microelectromechan. Sys.*, vol. 11, pp. 462-469, 2002.

[22] V. K. Pamula, P. Y. Paik, J. Venkatraman, M. G. Pollack, and R. B. Fair, "Microfluidic electrowetting-based droplet mixing," presented at Microelectromech. Systems Conference, Berkeley, CA, 2001.

[23] Y.-K. Lee, J. Deval, P. Tabeling, and C.-M. Ho, "Chaotic mixing in electrokinetically and pressure driven micr flow," presented at Proc. IEEE MEMs Workshop, Interlaken, Switzerland, 2001.

[24] H.-Y. Wu and C.-H. Liu, "A novel electrokinetic micromixer," presented at IEEE International Solid-State Sensors and Actuators Conference, Boston, MA, 2003.

[25] R. M. Moroney, R. M. White, and R. T. Howe, "Ultrasonically induced microtransport," presented at Proc. IEEE MEMs Workshop, Nara, Japan, 1991.

[26] H. Monnier, A. M. Wilhelm, and H. Delmas, "Effects of ultrasound on micromixing in flow cell," *Chem. Eng. Sci.*, vol. 55, pp. 4009-4020, 2000.

[27] Z. Yang, H. Goto, M. Matsumoto, and R. Maeda, "Ultrasonic micromixer for microfluidic systems," presented at IEEE Thirteenth Annual Int. Conf. on Micro Electro Mechanical Systems, Miyazaki, Japan, 2000.

[28] P. Woias, K. Hauser, and E. Yacoub-George, "An active silicon micromixer for μTAS applications," presented at Proc. Micro Total Analysis Systems, Enschede, Netherlands, 2000.

[29] N. T. Nguyen and R. M. White, "Acoustic streaming in micromachined flexural plate wave devices: Numerical simulation and experimental verification," *IEEE Trans. Ultrason., Ferroelectr., Freq. Cntrl.*, vol. 47, pp. 1463-1471, 2000.

[30] K. Miyamoto, S. Nagatomo, Y. Matsui, and S. Shiokawa, "Nonlinear vibration of liquid droplets by surface acoustic wave excitation," *Jpn. J. Appl. Phys.*, vol. 41, pp. 3465-3468, 2002.

[31] X. Zhu and E. S. Kim, "Microfluidic motion generation with acoustic waves," *Sensors and Actuators A. Phys*, vol. 66, pp. 355-360, 1998.

[32] Z. Yang, H. Goto, M. Matsumoto, and R. Maeda, "Active micromixer for microfluidic systems using lead-zirconate-titanate (PZT)-generated ultrasonic vibration," *Electrophoresis*, vol. 21, pp. 116-119, 2000.

[33] S. Shiokawa, Y. Matsui, and T. Ueda, "Liquid streaming and droplet formation caused by leaky rayleigh waves," presented at IEEE Ultrasonics Symposium, 1989.

[34] T. Uchida, T. Suzuki, and S. Shiokawa, "Investigation of acoustic streaming excited by surface acoustic waves," presented at IEEE Ultrasonics Symposium, Seattle, WA, 1995.

[35] D. Royer and E. Dieulesaint, *Elastic Waves in Solids I: Free and Guided Propagation*, vol. 1. Berlin: Springer, 2000.

[36] C. Caliendo, P. Imperatori, and E. Cianci, "Structural, morphological and acoustic properties of AlN thick films sputtered on Si(001) and Si(111) substrates at low temperature," *Thin Solid Films*, vol. 441, pp. 32-37, 2003.

[37] J. M. Ottino, *The Kinematics of Mixing: Stretching, Chaos and Transport*. New York: Cambridge University Press, 1989.

DISTRIBUTION LIST

10	MS 1425	Darren W. Branch
1	MS 9018	Central Technical Files, 8945-1
2	MS 0899	Technical Library, 9616
1	MS 1078	Steve Martin
1	MS 0892	Richard Cernosek
1	MS 1425	Grant D. Meyer
1	MS 0834	Chris Bourdon